

Supplementary Material: Impact of polyelectrolyte adsorption on the rheology of concentrated Poly(N-Isopropylacrylamide) microgel suspensions[†]

Rajam Elanchelian, Edouard Chauveau, and Domenico Truzzolillo*

*Laboratoire Charles Coulomb, UMR 5221, CNRS–Université de Montpellier, F-34095
Montpellier, France*

E-mail: domenico.truzzolillo@umontpellier.fr

Phone: +33 (0)467 143589

Light scattering

We report in figure 1 selected intensity autocorrelation functions ($g_2(t) - 1$) and time-averaged scattered intensity I/I_0 as a function of the squared modulus of the scattering vector q^2 at different temperatures. The lag time t (left panel) is normalized by $\eta_s/k_B T$ to filter out the trivial speeding up of the dynamics due to the temperature dependence of the solvent viscosity η_s and the thermal energy $k_B T$. I_0 is obtained by fitting $I(q)$ to the Guinier equation (eq. 4 of the main text). The autocorrelation functions and the scattered intensity data have been fitted by using respectively equation 3 and 4 (section 2.5 of the main manuscript) to extract the hydrodynamic radius (R_H) and gyration radius (R_g) as a function of temperature.

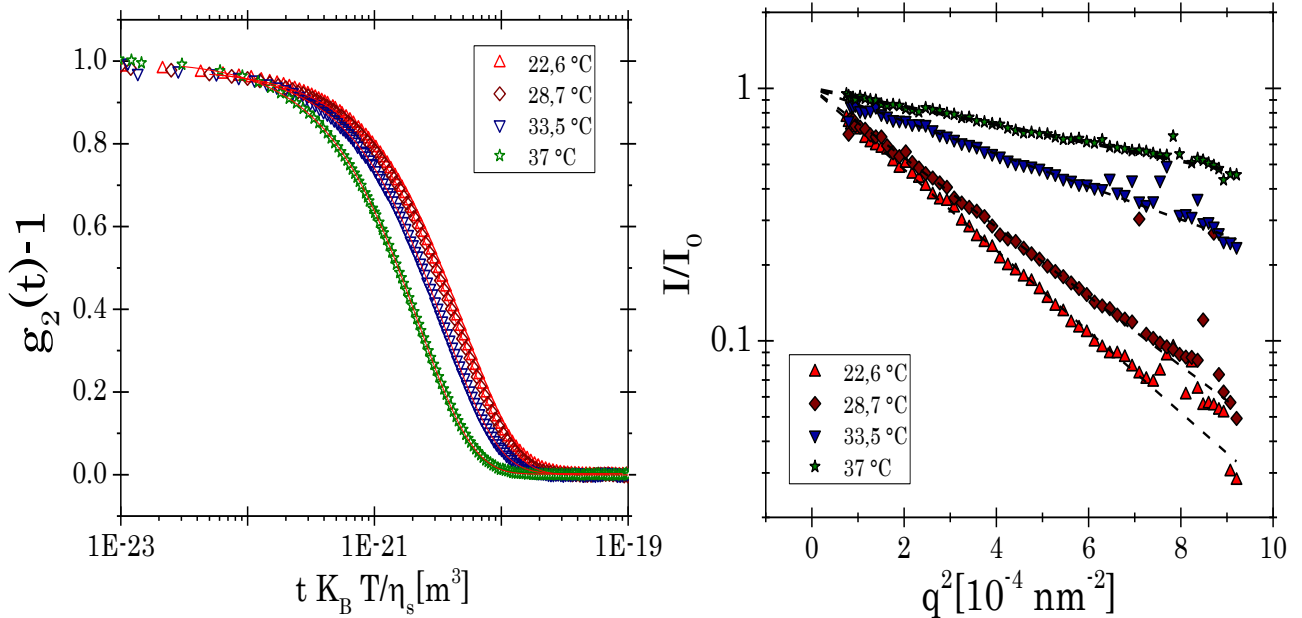


Figure 1: Autocorrelation functions $g_2 - 1$ (left panel) and normalized scattered intensity I/I_0 vs q^2 (right panel) at different temperatures as indicated in the panels. Red solid (black dashed) lines are cumulant (Guinier) fits according to equations 3 and 4 of the main manuscript for $g_2(t) - 1$ and I/I_0 respectively.

Viscosimetry

Figure 2 shows the viscosity ratio η/η_s for very dilute suspensions of bare microgels in the range $4.68 \cdot 10^{-5} < c(\text{wt}/\text{wt}) < 1.5 \cdot 10^{-3}$. The proportionality constant k between the generalized volume fraction φ and the mass fraction c of microgels has been obtained, as detailed in the main text, via a linear fit of the data to the Einstein equation.

Rheology of bare microgel suspensions

The rheology of bare microgels suspensions was investigated as a function of φ at $T=20$ °C to determine precisely the rheological state of the suspension in which PEs are progressively added. Figure 3 shows dynamic frequency (a) and strain (b) sweep tests performed in the

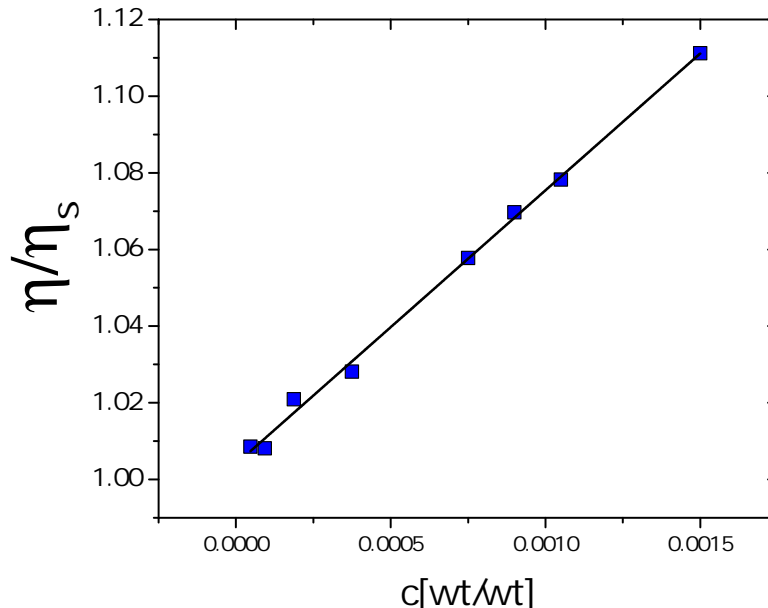


Figure 2: Viscosity ratio η/η_s for very dilute suspensions of microgels. The straight line is a linear fit of the data to the Einstein equation.

range $0.89 \leq \varphi \leq 1.57$. All samples show a solid-like response and a typical glassy behavior for $\varphi \geq 1.07$, with $G' > G''$ over about 3 decades in frequency and shallow minimum of G'' .^{1,2} Between $\varphi=1.07$ and $\varphi=0.89$ we observe a large drop of both the moduli, which flags the proximity to the rheological glass transition. The DSS tests confirm such a scenario with all the suspensions showing a nearly strain-independent first-harmonic moduli at low strains before non-linear behavior appears, with $G''(\gamma_0)$ reaching a maximum and then declining for $\varphi \geq 1.07$. The maximum of $G''(\gamma_0)$ is absent for $\varphi=0.89$ pointing to an important reduction of dissipative processes involved in the yielding transition. In all the cases a crossover between the two first harmonic moduli occurs and samples yield under oscillatory strain. The two insets show the storage modulus $G_p=G'(\omega=1 \text{ rad/s})$ (a) and the yield stress σ_y (b) at which the crossover $G'(\gamma_0) = G''(\gamma_0)$ occurs as a function of φ . The two quantities show an affine behavior with a drop of their values occurring between $\varphi=1.07$ and $\varphi=0.89$. Pellet and Cloitre³ have attributed such a sharp change to the passage from a thermal to a jammed glass of microgels, with the former being a solid whose elasticity is dominated by entropic

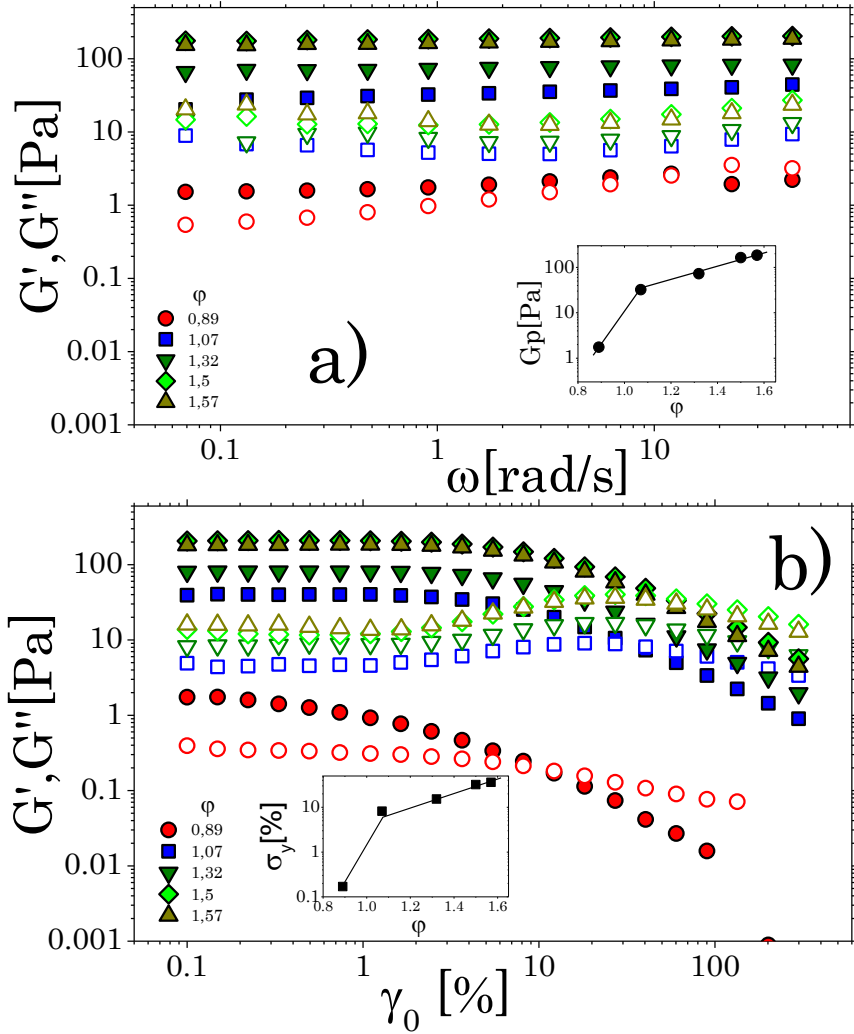


Figure 3: Storage modulus G' (solid symbols) and loss modulus G'' (open symbols) as a function of the oscillatory frequency ω (a) and respective first harmonic moduli as a function of the strain amplitude γ_0 at $\omega = 1$ rad/s (b) of concentrated PniPAM microgel suspensions at $T=20$ °C and different volume fractions as indicated in the panels. The insets show the plateau modulus G_p (a) and the yield stress σ_y (b) as a function of ϕ .

caging, while the latter is ruled by contact forces between particles and particle deformability. Therefore the microgel concentration that characterize the PE-microgel mixtures ($\varphi = 1.5$) is a jammed glass at $T=20$ °C. We show in the main manuscript (section 3.2) that at this number density, microgels form a gel when the suspension is heated up to $T=40$ °C.

Ageing of bare microgel suspensions

Prior to mixture preparation we performed a dynamic time sweep experiment to evaluate the aging of the bare concentrated microgel suspension ($\varphi = 1.5$, $\xi = 0$) over a time approximately equal to the duration of one whole experiment ($t \approx 2500$ s). Figure 4 shows the normalized storage and loss modulus ($G'/G'_{t=0}$, $G''/G''_{t=0}$) of the sample at $\omega = 2$ rad/s. The moduli did not show any remarkable evolution within this time window. This excludes that the changes of the moduli observed for the mixtures are due to different age of the pure microgel system.

Mobility

We report below the normalized mobility $\mu\eta/\epsilon$ for both the pure PE suspensions (Figure 5) and the PE-microgel mixtures (Figure 6). The data are the same shown in figures 4 and 7 of the main manuscript. For pure PE suspensions the normalized mobility does not show a visible trend for increasing temperature, indicating that the observed variation in absolute mobility is due mainly to the reduction of the solvent viscosity going 20 °C to 50 °C. We recall that in this temperature range the viscosity of water η_s decreases by a factor ≈ 1.85 , while the relative permittivity ϵ decreases by a factor ≈ 0.86 . By contrast the PE-microgel mixtures maintain the trend showed by the mobility μ (figure 7 of the main text), hence pointing to an important change of the charge density of the complexes upon varying temperature.

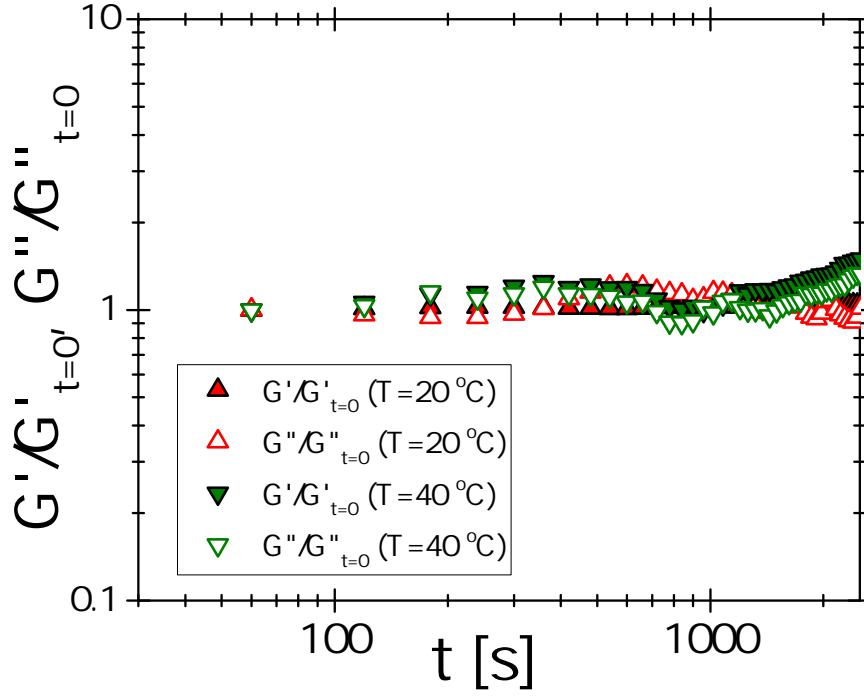


Figure 4: Normalized viscoelastic moduli ($\omega = 2$ rad/s) of the bare microgel suspension ($\varphi = 1.5$, $\xi = 0$) at $T=20^\circ\text{C}$ and $T=40^\circ\text{C}$ as indicated in the panels.

Table 1: Mobility in $\mu\text{m cm V/s}$ of PEs solutions and PE-microgel mixtures at $T=20^\circ\text{C}$ and $T=40^\circ\text{C}$ for the highest PE concentrations. Data are shown in figure 4 and figure 7 of the main manuscript. Data for pure microgel suspensions are also given for reference.

Sample code	$\mu(T=20^\circ\text{C})$	$\mu(T=40^\circ\text{C})$
M (No PE)	-1.52 ± 0.10	-3.20 ± 0.16
PLL ($C_{PE} = 1,25$ mg/ml)	3.46 ± 0.28	4.40 ± 0.66
M-PLL ($C_{PE} = 1,25$ mg/ml, $\xi = 0.5691$)	2.67 ± 0.16	5.94 ± 0.19
PSS ($C_{PE} = 1.75$ mg/ml)	-3.17 ± 0.44	-4.62 ± 0.36
M-PSS ($C_{PE} = 1.75$ mg/ml, $\xi = 0.645$)	-1.30 ± 0.18	-4.43 ± 0.19
PDADMAC ($C_{PE} = 1.38$ mg/ml)	2.42 ± 0.71	3.60 ± 0.40
M-PDADMAC ($C_{PE} = 1.38$ mg/ml, $\xi = 0.6625$)	1.42 ± 0.12	4.64 ± 0.18

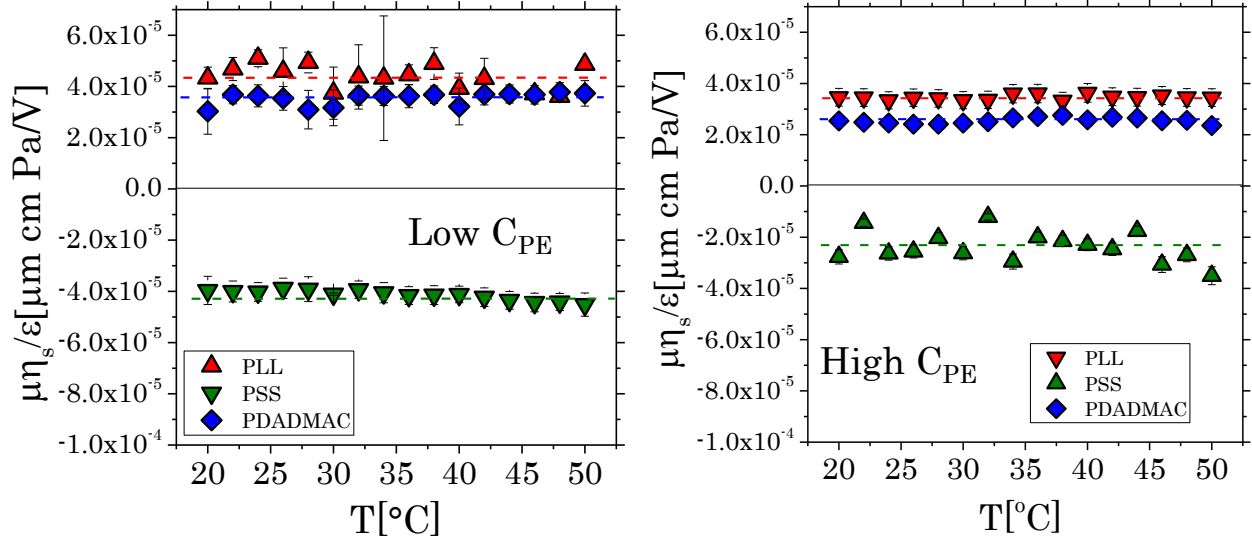


Figure 5: Normalized electrophoretic mobility of PLL at $C_{PE}=1.25$ mg/ml (left) and $C_{PE}=28$ mg/ml (right), PSS at $C_{PE}=1.75$ (left) and $C_{PE}=5.1$ (right), PDADMAC at $C_{PE}=1.38$ mg/ml (left) and $C_{PE}=35$ mg/ml (right) as a function of temperature.

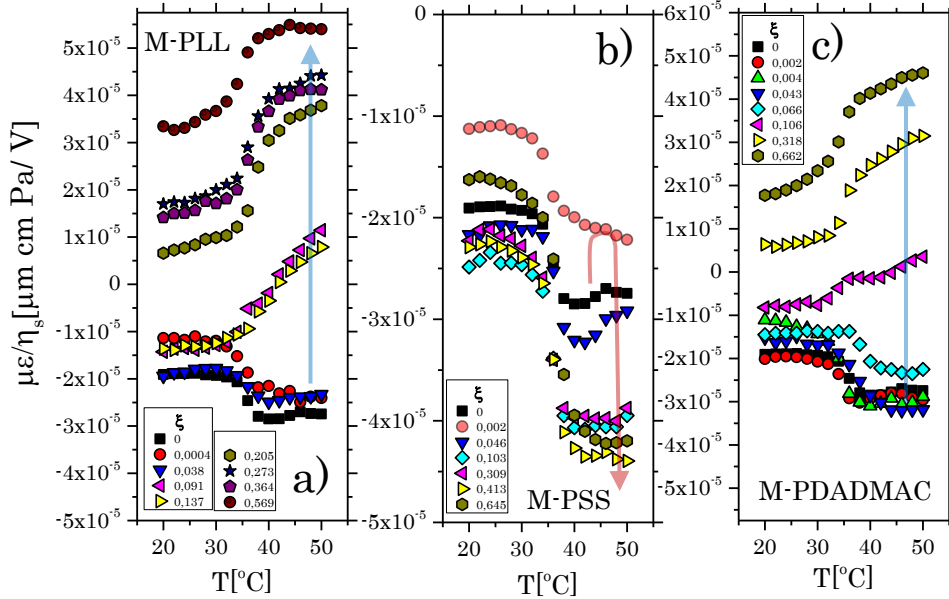


Figure 6: Normalized electrophoretic mobility of a) M-PLL, b) M-PSS and c) M-PDADMAC complexes at varying PE concentrations as a function of temperature. Data contains complementary samples that were not characterized via rheology. The colored arrows are a guide for the eye and point to the mobility variation from $\xi = 0$ up to the maximum PE concentration at $T > T_c^H$.

References

- (1) Sessoms, D. A.; Bischofberger, I.; Cipelletti, L.; Trappe, V. Multiple dynamic regimes in concentrated microgel systems. *Philosophical Transactions of the Royal Society A: Mathematical, Physical and Engineering Sciences* **2009**, *367*, 5013–5032.
- (2) Mewis, J.; Wagner, N. J. *Colloidal Suspension Rheology*, 1st ed.; Cambridge University Press, 2011.
- (3) Pellet, C.; Cloitre, M. The glass and jamming transitions of soft polyelectrolyte microgel suspensions. *Soft Matter* **2016**, *12*, 3710–3720.